PRAMANA
— journal of
physics

Vol. 70, No. 4
April 2008
pp. 617–632

Cold valleys in the radioactive decay of $^{248-254}$Cf isotopes

R K BIJU[1], SABINA SAHADEVAN[1], K P SANTHOSH[1,*] and ANTONY JOSEPH[2]

[1]P.G. Department of Physics and Research Centre, Payyanur College, Payyanur 670 327, India

[2]Department of Physics, Calicut University, Calicut 670 635, India

[*]Corresponding author. E-mail: kpsanthosh@eth.net; kps@calicutcity.com

MS received 30 July 2007; revised 9 October 2007; accepted 16 November 2007

Abstract. Based on the concept of cold valley in cold fission and fusion, we have investigated the cluster decay process in $^{248-254}$Cf isotopes. In addition to alpha particle minima, other deep minima occur for S, Ar and Ca clusters. It is found that inclusion of proximity potential does not change the position of minima but minima become deeper. Taking Coulomb and proximity potential as interacting barrier for post-scission region, we computed half-lives and other characteristics for various clusters from these parents. Our study reveals that these parents are stable against light clusters and unstable against heavy clusters. Computed half-lives for alpha decay agree with experimental values within two orders of magnitude. The most probable clusters from these parents are predicted to be ^{46}Ar, ^{48,50}Ca which indicate the role of doubly or near doubly magic clusters in cluster radioactivity. Odd A clusters are found to be favorable for emission from odd A parents. Cluster decay model is extended to symmetric region and it is found that symmetric fission is also probable which stresses the role of doubly or near doubly magic ^{132}Sn nuclei. Geiger–Nuttal plots were studied for various clusters and are found to be linear with varying slopes and intercepts.

Keywords. Cluster decay; alpha decay.

PACS Nos 23.70.+j; 25.85.Ca; 27.90.+b

1. Introduction

The spontaneous decay of radioactive nuclei with the emission of fragments heavier than alpha particle is termed as cluster radioactivity. The phenomenon of cluster radioactivity was predicted towards the end of 1970s by Sandulescu *et al* [1] on the basis of quantum mechanical fragmentation theory (QMFT). In 1984, Rose and Jones [2] confirmed this in the radioactive decay of ^{14}C from ^{223}Ra. Since then the ^{14}C decay of many isotopes of Ra nuclei, and many other heavy cluster decays have been observed. Also ^{24}Ne from ^{230}Th, ^{231}Pa, ^{232}U, ^{20}O from ^{228}Th, ^{28,30}Mg from ^{238}Pu, ^{32,34}Si from ^{238}Pu and ^{241}Am have been observed [3]. From these decays the

half-lives and branching ratios with respect to alpha decay are measured. Knowing that radioactive nuclei also fission spontaneously, this new phenomenon can either be described as a strong asymmetric fission [4] or an exotic process of cluster formation and escape from the parent nucleus by making many assaults on the confining barrier similar to alpha decay [5]. This is because although the physics of the two approaches is apparently different, they are actually almost similar. Interpreting the cluster preformation probability within a super asymmetric fission model as the penetrability of pre-scission part of the barrier, it was shown that the preformed cluster model is in fact, equivalent to the super asymmetric fission model [6–8]. We would like to mention that we have calculated cluster formation probability P_0, within our fission model [9] and found that P_0 decreases with increase in mass of cluster up to $A_2 = 20$ and then remains a constant, i.e. the transition from cluster mode to fission mode takes place at $A_2 = 20$.

In the present paper, we have studied the cold valleys in the cluster radioactivity of $^{248-254}$Cf isotopes based on the concept of cold valley description of cold fission and fusion. The californium nucleus offers interesting possibilities for heavy cluster decay studies, since the closed shell effects of the doubly magic ^{48}Ca nucleus are expected to come into play. So far it was the closed shell effects of the daughter nucleus (^{208}Pb or ^{100,132}Sn) that has been observed [3,10] or predicted [11–14]. Another interesting possibility is that of ^{252}Cf since both spontaneous binary and ternary fission has already been observed by triple gamma coincidence technique with gamma sphere having 72 gamma-ray detectors [15–19].

Californium was first synthesized in 1950 by bombarding microgram quantities of ^{242}Cm with 35 MeV helium ions in the Berkeley 60-inch cyclotron. Nineteen isotopes of californium have been characterized, the most stable among them being ^{251}Cf with a half-life of 898 years, ^{249}Cf with a half-life of 351 years, and ^{250}Cf with a half-life of 13 years. All the remaining radioactive isotopes have half-lives that are less than 2.7 years, majority of them being shorter than 20 min. The existence of the isotopes $^{249-252}$Cf makes it feasible to isolate californium in weighable amounts so that its properties can be investigated with macroscopic quantities.

In the fission of ^{252}Cf, about 100 different final fragments are produced [15]. During the fission process two primary fragments along with several neutrons and/or light clusters are emitted. Another point is the theoretical confirmation of the existence of two distinct regions of ^{252}Cf cold fission, the first extending from the mass split 96/156 up to 114/138 and the second one comprising only a narrow mass range around the mass split 120/132. Here the shell closure of neutrons or protons does not seem to be involved. Although shell effects should play an important role in the odd–even differences by enhancing the odd–odd mass splits with respect to the even–even one, this result emphasizes that the fragments are emitted with deformations corresponding to that of the ground state. The spherical region gives only a hint of the importance of the magic nucleus ^{132}Sn which is susceptible to be produced in a heavy cluster process, similar to that of light clusters [20]. In the case of cold alpha-ternary fission [21] of ^{252}Cf, the correlation between two even-Z fragments with sum of charges $Z = 96$ and sum of masses $A = 248$ (for e.g. ^{146}Ba and ^{102}Zr) is involved.

We have studied the cluster radioactivity of $^{248-254}$Cf based on the potential barrier determined by two-sphere approximation, as the sum of Coulomb and

nuclear proximity potential [22] for the touching and separated configurations ($z > 0$). Here z is the distance between the near surfaces of the fragments. For the overlap region ($z < 0$), we used simple power-law interpolation. The possibility to have a cluster decay process is

$$Q = M(A, Z) - M(A_1, Z_1) - M(A_2, Z_2) > 0, \tag{1}$$

where $M(A, Z), M(A_1, Z_1)$ and $M(A_2, Z_2)$ are the atomic masses of the parent, daughter and cluster respectively. Section 2 describes the features of the model and §3 contains the results, discussion and conclusion.

2. The model

The interacting potential barrier for a parent nucleus exhibiting exotic decay is given by

$$V = \frac{Z_1 Z_2 e^2}{r} + V_{\mathrm{p}}(z) + \frac{\hbar^2 l(l+1)}{2\mu r^2}, \quad \text{for } z > 0. \tag{2}$$

Here Z_1 and Z_2 are the atomic numbers of daughter and emitted cluster, r is the distance between fragment centers, ℓ is the angular momentum, μ is the reduced mass and V_{p} is the proximity potential given by Blocki *et al* [23]

$$V_{\mathrm{p}}(z) = 4\pi\gamma b \left[\frac{C_1 C_2}{(C_1 + C_2)}\right] \Phi\left(\frac{z}{b}\right). \tag{3}$$

With the nuclear surface tension coefficient,

$$\gamma = 0.9517[1 - 1.7826(N - Z)^2/A^2] \text{ MeV/fm}^2, \tag{4}$$

where N, Z and A represent neutron, proton and mass numbers of parent. Φ represents the universal proximity potential given as [24]

$$\Phi(\varepsilon) = -4.41\mathrm{e}^{-\varepsilon/0.7176}, \quad \text{for } \varepsilon \geq 1.9475 \tag{5}$$

$$\Phi(\varepsilon) = -1.7817 + 0.9270\varepsilon + 0.0169\varepsilon^2 - 0.05148\varepsilon^3, \quad \text{for } 0 \leq \varepsilon \leq 1.9475. \tag{6}$$

With $\varepsilon = z/b$, where the width (diffuseness) of the nuclear surface $b \approx 1$ and Siissmann central radii C_i of fragments related to sharp radii R_i is

$$C_i = R_i - \left(\frac{b^2}{R_i}\right). \tag{7}$$

For R_i we use semi-empirical formula in terms of mass number A_i as [23]

$$R_i = 1.28A_i^{1/3} - 0.76 + 0.8A_i^{-1/3}. \tag{8}$$

Using one-dimensional WKB approximation, the barrier penetrability P is given as

$$P = \exp\left\{-\frac{2}{\hbar}\int_a^b \sqrt{2\mu(V-Q)}\mathrm{d}z\right\}. \tag{9}$$

Here the mass parameter is replaced by $\mu = mA_1A_2/A$, where m is the nucleon mass and A_1, A_2 are the mass numbers of daughter and emitted cluster respectively. The turning points a and b are determined from the equation $V(a) = V(b) = Q$, whose solutions provide three turning points. The fragments (emitted cluster and daughter nuclei) oscillate between the first and second turning points and tunnels through the barrier at second turning point a and third turning point b. The above integral can be evaluated numerically or analytically, and the half-life time is given by

$$T_{1/2} = \left(\frac{\ln 2}{\lambda}\right) = \left(\frac{\ln 2}{\upsilon P}\right), \tag{10}$$

where $\upsilon = (\omega/2\pi) = (2E_\mathrm{v}/h)$ represent the number of assaults on the barrier per second and λ the decay constant. E_v, the empirical zero-point vibration energy is given as [25]

$$E_\mathrm{v} = Q\left\{0.056 + 0.039\exp\left[\frac{(4-A_2)}{2.5}\right]\right\}, \quad \text{for } A_2 \geq 4. \tag{11}$$

3. Results, discussion and conclusion

The concept of cold valley was introduced in relation to the structure of minima in the so-called driving potential, which is defined as the difference between the interaction potential and the decay energy (Q value) of the reaction. Q values are

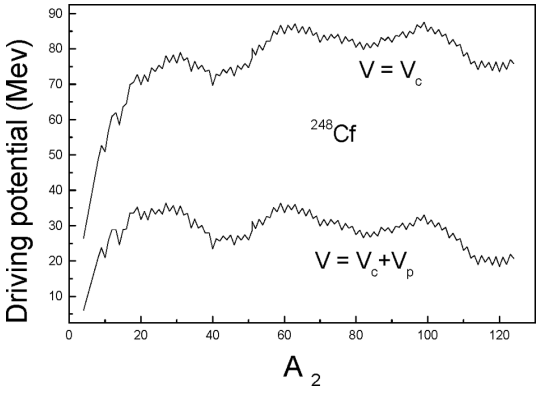

Figure 1. The plot of driving potential vs. A_2, mass of one fragment for ^{248}Cf isotope. The calculations are made for touching configuration, $r = C_1 + C_2$.

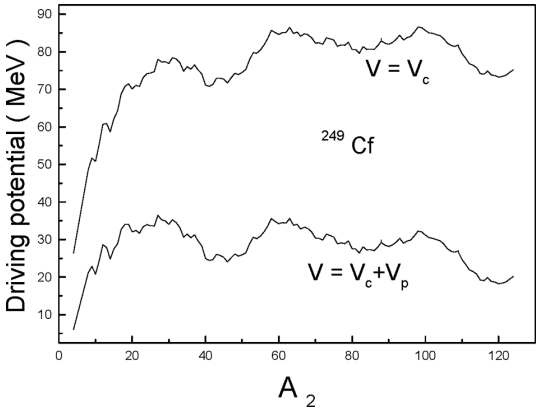

Figure 2. The plot of driving potential vs. A_2, mass of one fragment for ^{249}Cf isotope. The calculations are made for touching configuration, $r = C_1 + C_2$.

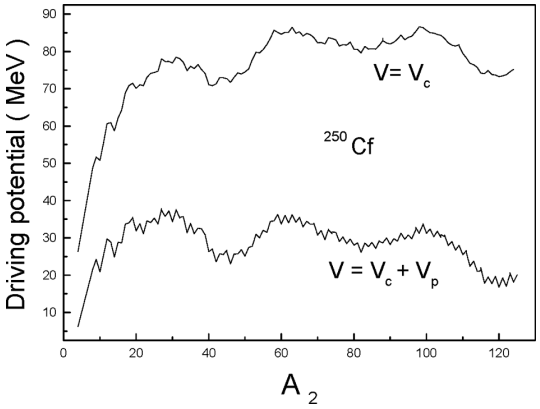

Figure 3. The plot of driving potential vs. A_2, mass of one fragment for ^{250}Cf isotope. The calculations are made for touching configuration, $r = C_1 + C_2$.

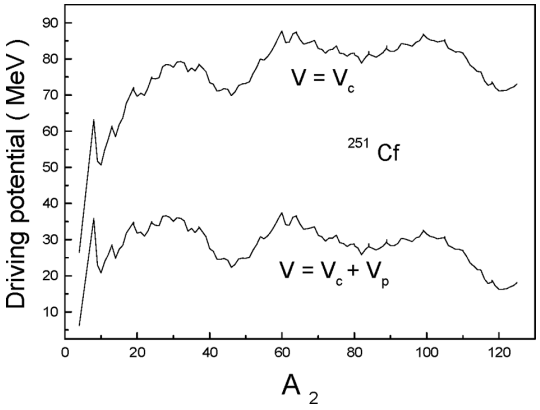

Figure 4. The plot of driving potential vs. A_2, mass of one fragment for ^{251}Cf isotope. The calculations are made for touching configuration, $r = C_1 + C_2$.

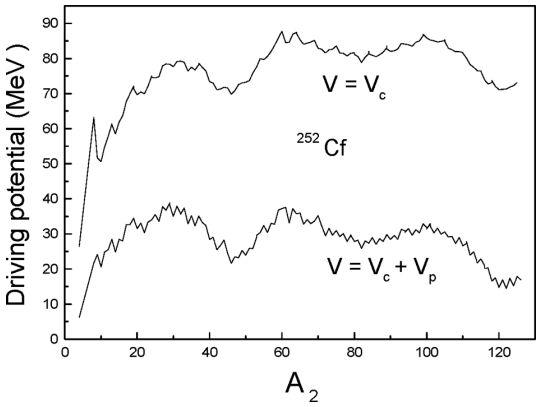

Figure 5. The plot of driving potential vs. A_2, mass of one fragment for ^{252}Cf isotope. The calculations are made for touching configuration, $r = C_1 + C_2$.

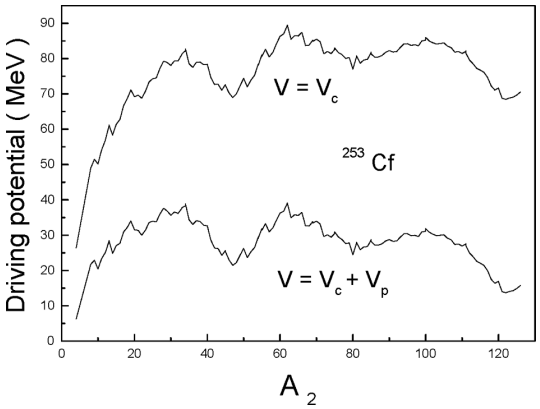

Figure 6. The plot of driving potential vs. A_2, mass of one fragment for ^{253}Cf isotope. The calculations are made for touching configuration, $r = C_1 + C_2$.

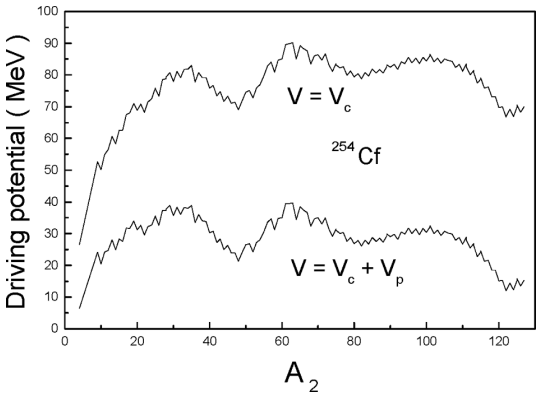

Figure 7. The plot of driving potential vs. A_2, mass of one fragment for ^{254}Cf isotope. The calculations are made for touching configuration, $r = C_1 + C_2$.

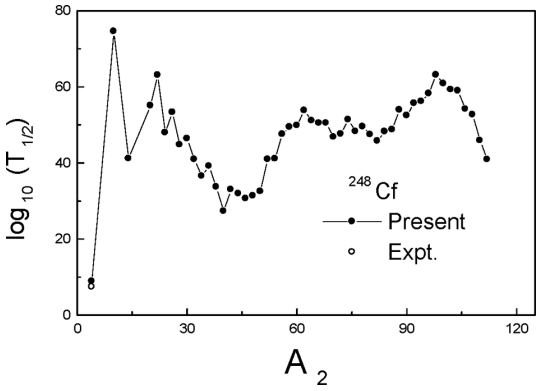

Figure 8. Plot of the computed $\log_{10}(T_{1/2})$ vs. mass A_2 for ^{248}Cf isotopes.

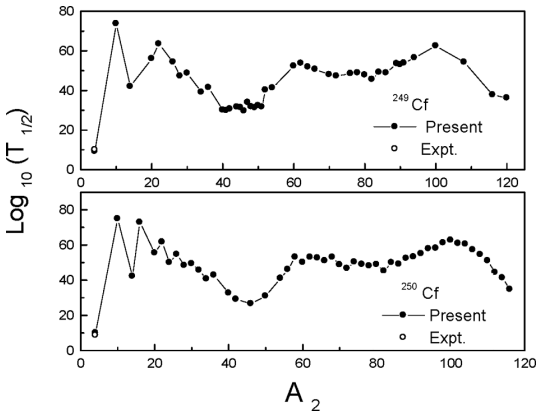

Figure 9. Plot of the computed $\log_{10}(T_{1/2})$ vs. mass A_2 for ^{249,250}Cf isotopes.

computed using experimental binding energies of Audi and Wapstra [26]. The interaction potential is a function of distance of separation of interacting fragments. The driving potential of the compound nucleus is calculated for all possible cluster–daughter combinations as a function of mass and charge asymmetries, $\eta = \frac{A_1-A_2}{A_1+A_2}$ and $\eta_z = \frac{Z_1-Z_2}{Z_1+Z_2}$ for the touching configuration of the fragments, i.e the distance between the fragments $r = C_1 + C_2$, where C_1 and C_2 are the Siissmann central radii. The charges of the fragments are fixed by minimizing the driving potential for fixed η and r. In the charge asymmetric coordinate η_z, i.e. for every fixed mass pair (A_1, A_2) a single pair of charges is determined among all possible combinations. The occurrence of cold valleys for mass asymmetric combinations is due to the shell effect of one or both fragments. The cluster emission is energetically possible when Q value of the reaction is greater than zero (eq. (1)). For example, from ^{248}Cf parent eight clusters with different Z values and with the same $A_2 = 50$ are possible for emission with Q value varying from 87.54 MeV (for ^{50}Cl) to 137.59 MeV (for ^{50}Sc). The peak in Q value corresponds to a dip in the driving

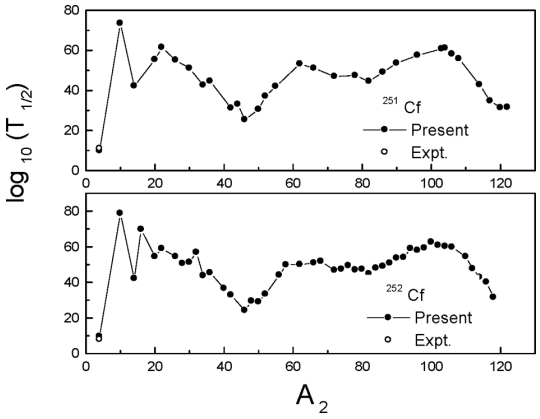

Figure 10. Plot of the computed $\log_{10}(T_{1/2})$ vs. mass A_2 for ^{251,252}Cf isotopes.

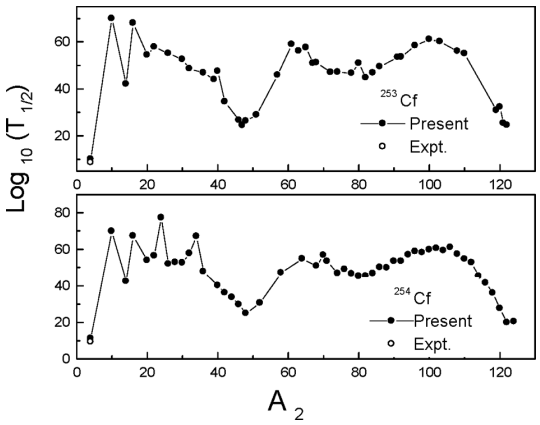

Figure 11. Plot of the computed $\log_{10}(T_{1/2})$ vs. mass A_2 for ^{253,254}Cf isotopes.

potential and correspondingly high barrier penetrability according to eq. (9). So ^{50}Sc which has minimum driving potential is most probable for emission. But our calculation shows ^{50}Ca ($Q = 136.7$ MeV) has minimum driving potential instead of ^{50}Sc. This is due to the shell effect of the cluster. Also our calculation shows that cluster formation probability is maximum for ^{50}Ca compared to other clusters. So ^{50}Ca which is in the cold valley is most probable for emission with $T_{1/2} = 3.36\times 10^{32}$ s, near the present experimental limit for measurements. So there is no need to compute decay half-lives for other clusters. Again cold valley plays an important role in the shell closure of daughter nuclei. For e.g. in the case of ^{250}Cf with $A_2 = 42$ the Q value varies from 73.649 MeV (for ^{42}Si) to 118.686 MeV (for ^{42}Ar). But the deepest minima in driving potential is obtained for ^{42}S ($Q = 110.13$ MeV) instead of ^{42}Ar. This stresses the role of doubly magic ^{208}Pb daughter nuclei. The half-life for ^{42}S cluster is $T_{1/2} = 1.297 \times 10^{29}$ s, which is well within the present

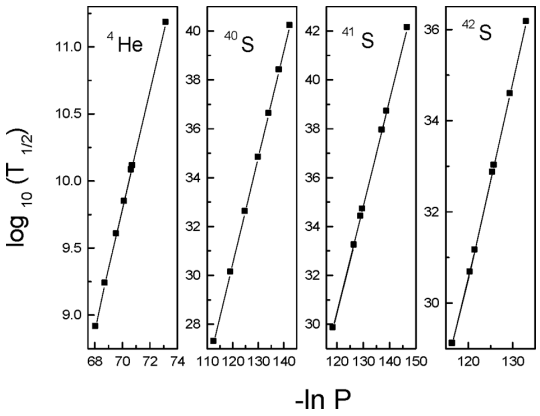

Figure 12. Geiger–Nuttal plots of $\log_{10}(T_{1/2})$ vs. – ln P for ^{4}He and $^{40-42}$S emitting from various californium isotopes.

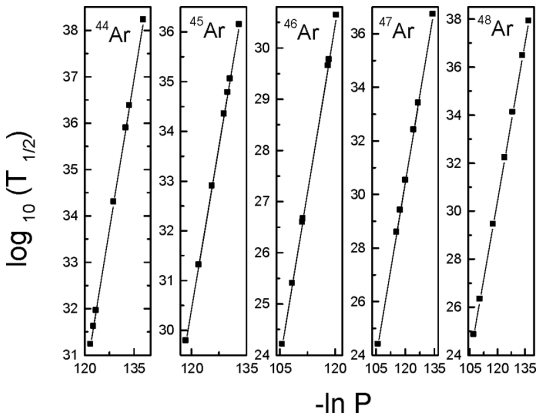

Figure 13. Geiger–Nuttal plots of $\log_{10}(T_{1/2})$ vs. – ln P for $^{44-48}$Ar emitting from various californium isotopes.

experimental limit for measurements. Figures 1–7 represent the plots of driving potential vs. A_2, mass of one fragment for ^{248}Cf to ^{254}Cf, with and without including proximity potential. The minima in potential energy curve represent the most probable decay. From these potential energy curves, it is clear that inclusion of proximity potential does not change the position of minima, but become deeper.

The proximity potential was first used by Shi and Swiatecki [27] in an empirical manner and has been quite extensively used over a decade by Malik and Gupta [28] in the preformed cluster model (PCM) which is based on pocket formula of Blocki *et al* [23] given as

$$\Phi(\varepsilon) = -\left(\frac{1}{2}\right)(\varepsilon - 2.54)^2 - 0.0852(\varepsilon - 2.54)^3, \quad \text{for } \varepsilon \leq 1.2511 \qquad (12)$$

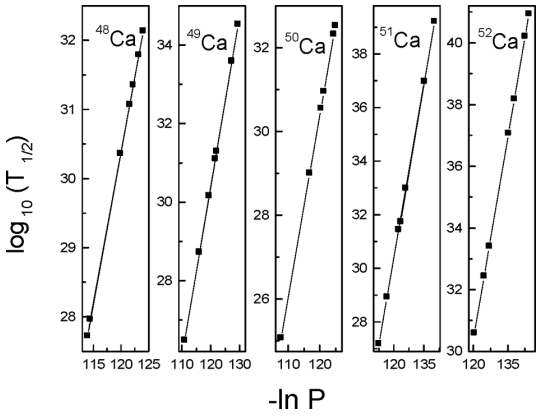

Figure 14. Geiger–Nuttal plots of $\log_{10}(T_{1/2})$ vs. – ln P for $^{48-52}$Ca emitting from various californium isotopes.

$$\Phi(\varepsilon) = -3.437 \exp\left(\frac{-\varepsilon}{0.75}\right), \quad \text{for } \varepsilon \geq 1.2511. \tag{13}$$

In the present model, another formulation of proximity potential [24] is used as given by eqs (5) and (6). In this model cluster formation probability is taken as unity for all clusters irrespective of their masses, and so the present model differs from PCM by a factor P_0, the cluster formation probability. In the present model, assault frequency ν is calculated for each parent–cluster combination which is associated with zero-point vibration energy. But Shi and Swiatecki [27] get ν empirically, unrealistic values 10^{22} for even A parent and 10^{20} for odd A parent.

Figures 8–11 represent the computed $\log_{10}(T_{1/2})$ vs. A_2 plots for $^{248-254}$Cf. The angular momentum ℓ carried away in decay process, appearing in eq. (2) is often low which is decided by the spin parity conservation. In the present work, calculations are done assuming zero angular momentum transfers. Our study reveals that $^{248-254}$Cf nuclei are stable against light clusters but unstable against heavy clusters ($A_2 \geq 40$). The calculated alpha decay half-life time values for $^{248-254}$Cf match the experimental values within two orders of magnitude (e.g. in ^{248}Cf experimental $\log_{10}(T_{1/2}) = 7.42$ and present value = 8.91; in ^{249}Cf experimental $\log_{10}(T_{1/2}) = 10.04$ and present value = 9.24). The experimental alpha half-lives are taken from [29]. ^{40}S, ^{46}Ar from ^{248}Cf; ^{42}S, ^{46}Ar, ^{50}Ca from ^{250}Cf; ^{46,47,48}Ar, ^{48,49,50}Ca from ^{252}Cf; ^{46,47,48}Ar, ^{50,51,52}Ca from ^{254}Cf are the most probable for decay with $T_{1/2} < 10^{30}$ s. Another point is that odd A clusters are also probable from odd A parents (e.g. ^{41}S, ^{45}Ar, ^{49,51}Ca from ^{249}Cf, ^{45,47}Ar, ^{49,51}Ca from ^{251}Cf and ^{47}Ar, ^{49}Ca, ^{51}Ca from ^{253}Cf). We would like to point out that in cluster radioactivity the only odd A cluster so far observed is ^{23}F from ^{231}Pa [30]. The computed half-life time values for various clusters from ^{249,252}Cf isotopes are in agreement with the values reported by Balasubramaniam and Gupta [31] based on PCM and with microscopic super asymmetric fission model [32].

Tables 1 and 2 show half-life time and other characteristics for the most probable cluster emission (with $T_{1/2} < 10^{30}$ s) and branching ratio with respect to alpha

Table 1. Logarithm of predicted half-life time, branching ratio and other characteristics of $^{248-251}$Cf isotopes decaying by the emission of most probable clusters. The calculations are done with zero angular momentum transfers.

Parent nuclei	Emitted cluster	Daughter nuclei	Q-value (MeV)	Penetrability P	Decay constant	$\log_{10}(T_{1/2})$	Branching ratio
^{248}Cf	^{4}He	^{244}Cm	6.36	2.889 e-30	8.443 e-10	8.91	–
	^{40}S	^{208}Pb	111.85	1.168 e-49	3.539 e-28	27.29	1.473 e-20
	^{44}Ar	^{204}Hg	124.20	2.247 e-54	7.559 e-33	31.96	3.146 e-25
	^{46}Ar	^{202}Hg	124.32	4.733 e-53	1.593 e-31	30.64	6.632 e-24
	^{48}Ca	^{200}Pt	138.07	8.202 e-54	3.067 e-32	31.35	1.276 e-24
	^{50}Ca	^{198}Pt	136.73	5.574 e-55	2.064 e-33	32.53	8.590 e-26
^{249}Cf	^{4}He	^{245}Cm	6.23	1.384 e-30	4.003 e-10	9.24	–
	^{40}S	^{209}Pb	110.20	1.716 e-52	5.122 e-31	30.31	8.104 e-21
	^{41}S	^{208}Pb	110.08	3.242 e-52	9.666 e-31	29.86	1.529 e-20
	^{42}S	^{207}Pb	109.39	4.893 e-53	1.449 e-31	30.68	2.293 e-21
	^{44}Ar	^{205}Hg	124.29	4.976 e-54	1.675 e-32	31.62	2.650 e-22
	^{45}Ar	^{204}Hg	124.15	9.993 e-54	3.359 e-32	31.31	5.316 e-22
	^{46}Ar	^{203}Hg	124.72	4.583 e-52	1.548 e-30	29.65	2.450 e-20
	^{47}Ar	^{202}Hg	122.99	8.183 e-55	2.730 e-33	32.41	4.313 e-23
	^{48}Ca	^{201}Pt	137.69	3.023 e-54	1.127 e-32	31.79	1.784 e-22
	^{49}Ca	^{200}Pt	137.63	9.464 e-54	3.528 e-32	31.29	5.582 e-22
	^{50}Ca	^{199}Pt	136.72	8.948 e-55	3.313 e-33	32.32	5.242 e-23
	^{51}Ca	^{198}Pt	136.72	3.454 e-54	1.278 e-32	31.73	2.024 e-22
^{250}Cf	^{4}He	^{246}Cm	6.13	1.886 e-30	5.311 e-11	10.11	–
	^{40}S	^{210}Pb	108.76	5.731 e-55	1.688 e-33	32.61	1.193 e-24
	^{42}S	^{208}Pb	110.13	1.791 e-51	5.343 e-30	29.11	3.775 e-21
	^{44}Ar	^{206}Hg	124.39	1.205 e-53	4.059 e-32	31.23	2.869 e-23
	^{45}Ar	^{205}Hg	123.19	2.615 e-55	8.723 e-34	32.90	6.165 e-25
	^{46}Ar	^{204}Hg	125.59	5.227 e-49	1.778 e-27	26.59	1.257 e-18
	^{48}Ca	^{202}Pt	137.98	1.581 e-53	5.910 e-32	31.07	4.177 e-23
	^{50}Ca	^{200}Pt	137.36	2.071 e-53	7.704 e-32	30.95	5.445 e-23
^{251}Cf	^{4}He	^{247}Cm	6.18	3.477 e-31	9.863 e-11	9.85	–
	^{42}S	^{209}Pb	108.96	1.618 e-53	4.774 e-32	31.16	5.600 e-21
	^{45}Ar	^{206}Hg	124.81	4.516 e-52	4.540 e-28	29.78	1.336 e-19
	^{46}Ar	^{205}Hg	126.15	8.150 e-48	2.785 e-26	25.40	3.266 e-15
	^{47}Ar	^{204}Hg	124.75	5.306 e-51	1.792 e-29	28.59	2.105 e-18
	^{48}Ar	^{203}Hg	122.61	1.265 e-54	4.201 e-33	32.22	4.927 e-22
	^{48}Ca	^{203}Pt	139.73	3.094 e-50	1.171 e-28	27.77	1.373 e-17
	^{49}Ca	^{202}Pt	138.02	1.266 e-52	4.733 e-31	30.17	5.551 e-20
	^{50}Ca	^{201}Pt	137.46	5.234 e-53	1.948 e-31	30.55	2.285 e-20
	^{51}Ca	^{200}Pt	136.64	6.702 e-54	2.480 e-32	31.45	2.909 e-21

decay, from various californium nuclei and table 3 gives the details of the most probable spontaneous symmetric fission.

The first isotope of californium that we considered is ^{248}Cf. The deepest minimum corresponds to the splitting of ^{40}S + ^{208}Pb. The cluster is predicted by the

Table 2. Logarithm of predicted half-life time, branching ratio and other characteristics of $^{252-254}$Cf isotopes decaying by the emission of the most probable clusters. The calculations are done with zero angular momentum transfers.

Parent nuclei	Emitted cluster	Daughter nuclei	Q-value (MeV)	Penetrability P	Decay constant	$\log_{10}(T_{1/2})$	Branching ratio
^{252}Cf	^{4}He	^{248}Cm	6.22	6.017 e-31	1.719 e-10	9.61	
	^{42}S	^{210}Pb	107.97	3.190 e-55	9.329 e-34	32.87	1.340 e-25
	^{46}Ar	^{206}Hg	126.71	1.247 e-46	4.281 e-25	24.21	6.177 e-17
	^{47}Ar	^{205}Hg	124.24	7.990 e-52	2.688 e-30	29.41	3.897 e-22
	^{48}Ar	^{204}Hg	123.94	7.271 e-52	2.440 e-30	29.45	3.520 e-22
	^{48}Ca	^{204}Pt	139.50	1.983 e-50	7.492 e-29	27.97	1.081 e-20
	^{49}Ca	^{203}Pt	138.71	3.488 e-51	1.310 e-29	28.72	1.288 e-21
	^{50}Ca	^{202}Pt	138.20	1.841 e-51	6.891 e-30	29.00	9.944 e-32
	^{51}Ca	^{201}Pt	135.68	1.945 e-55	7.746 e-34	32.99	1.031 e-25
^{253}Cf	^{4}He	^{249}Cm	6.13	2.034 e-31	5.725 e-11	10.08	
	^{46}Ar	^{207}Hg	125.25	4.458 e-49	1.512 e-27	26.66	1.145 e-18
	^{47}Ar	^{206}Hg	126.17	8.041 e-47	2.748 e-25	24.10	2.081 e-16
	^{48}Ar	^{205}Hg	124.80	9.685 e-49	3.273 e-27	26.33	2.479 e-18
	^{48}Ca	^{205}Pt	138.03	8.080 e-53	3.212 e-31	30.36	2.288 e-22
	^{49}Ca	^{204}Pt	139.85	6.034 e-49	2.285 e-27	26.48	1.731 e-18
	^{50}Ca	^{203}Pt	140.26	1.548 e-47	5.878 e-26	25.07	4.452 e-17
	^{51}Ca	^{202}Pt	137.79	2.221 e-51	8.286 e-30	28.92	6.275 e-21
^{254}Cf	^{4}He	^{250}Cm	5.93	1.667 e-32	4.539 e-12	11.18	
	^{46}Ar	^{208}Hg	124.16	3.497 e-52	1.176 e-30	29.77	3.464 e-21
	^{47}Ar	^{207}Hg	123.48	6.211 e-53	2.077 e-31	30.52	6.119 e-22
	^{48}Ar	^{206}Hg	125.46	2.832 e-47	9.624 e-26	24.86	2.835 e-16
	^{48}Ca	^{206}Pt	136.92	1.362 e-54	5.051 e-33	32.14	1.488 e-23
	^{49}Ca	^{205}Pt	137.15	1.469 e-53	5.458 e-32	31.10	1.608 e-22
	^{50}Ca	^{204}Pt	140.17	1.755 e-47	6.661 e-26	25.11	1.962 e-16
	^{51}Ca	^{203}Pt	138.62	1.193 e-49	4.480 e-28	27.19	1.320 e-18
	^{52}Ca	^{202}Pt	136.44	4.738 e-53	1.751 e-31	30.60	1.157 e-22

macroscopic–microscopic model [33] to be prolate deformed ($\beta_2 = 0.254$) which sensitively lowers the barrier. The lowest half-life time (deepest minima in cold valley) for ^{41}S from ^{249}Cf and ^{42}S from ^{250}Cf shows the role of doubly magic ^{208}Pb daughter and lowest half-life time for ^{46}Ar from ^{251,252}Cf, ^{47}Ar from ^{253}Cf and ^{48}Ar from ^{254}Cf shows the role of near doubly magic ^{206}Hg daughter. From tables 1 and 2, ^{48}Ca from all californium isotopes are favorable for emission with $T_{1/2}$ between 10^{27} s and 10^{32} s, which are near and within the present limits for experiments. This stresses the role of doubly magic cluster ($N = 28, Z = 20$) in decay process. Minima for ^{46}Ar (near doubly magic cluster with $N = 28$, $Z = 18$) from ^{249}Cf ($T_{1/2} \sim 10^{29}$ s) and from ^{250}Cf ($T_{1/2} \sim 10^{26}$ s) show that these clusters are also favorable for emission. Branching ratio calculation also reveals that ^{46}Ar, ^{50}Ca are favorable for emission from these parents. We would like to point out that with presently

Table 3. Logarithm of predicted half-life time and other characteristics of the most spontaneous symmetric fission from $^{248-254}$Cf isotopes. The calculations are done with zero angular momentum transfers.

Parent nuclei	Decay mode	Q-value (MeV)	Penetrability P	Decay constant (s^{-1})	$\log_{10}(T_{1/2})$
^{251}Cf	^{120}Cd + ^{131}Sn	235.491	4.89 e-54	3.120 e-32	31.35
	^{122}Cd + ^{129}Sn	235.328	3.12 e-54	1.990 e-32	31.55
^{252}Cf	^{118}Pd + ^{134}Te	233.898	3.09 e-54	1.960 e-32	31.55
^{253}Cf	^{119}Pd + ^{134}Te	233.695	1.39 e-53	8.790 e-32	30.90
	^{121}Cd + ^{132}Sn	236.975	4.66 e-48	2.993 e-26	25.36
	^{122}Cd + ^{131}Sn	237.260	3.31 e-47	2.126 e-25	24.51
^{254}Cf	^{122}Cd + ^{132}Sn	238.530	1.35 e-42	8.713 e-21	19.90
	^{124}Cd + ^{130}Sn	238.295	4.64 e-43	2.996 e-21	20.36
	^{120}Pd + ^{134}Te	234.540	2.37 e-50	1.504 e-28	27.66

Table 4. Shows slopes and intercepts of Geiger–Nuttal plots for different clusters emitted from various Cf isotopes.

Emitted cluster	Slope X	Intercept Y
^{4}He	159.5794	−54.37071
^{40}S	3882.5872	−339.74358
^{41}S	3959.7085	−347.37920
^{42}S	3867.4960	−339.21955
^{44}Ar	4382.8412	−361.52451
^{45}Ar	4613.4314	−382.87440
^{46}Ar	7038.5684	−601.31608
^{47}Ar	6191.8714	−526.32963
^{48}Ar	5498.2720	−464.25431
^{48}Ca	5656.4006	−450.69245
^{49}Ca	6418.3779	−516.25389
^{50}Ca	6800.7934	−549.32136
^{51}Ca	7575.7490	−611.37097
^{52}Ca	9981.6157	−826.07409

available experimental techniques, branching ratio up to 10^{-19} are possible for measurement [34]. Our decay calculation shows that symmetric fission is also probable in ^{251}Cf (e.g. ^{120,122}Cd + ^{131,129}Sn), ^{253}Cf (e.g. ^{119}Pd + ^{134}Te, ^{121,122}Cd + ^{132,131}Sn) and ^{254}Cf (e.g. ^{122,124}Cd + ^{132,130}Sn). This also stresses the role of doubly or near doubly magic ^{132}Sn nuclei.

Figures 12–14 represent Geiger–Nuttal plots of $\log_{10}(T_{1/2})$ vs. – ln P for ^{4}He, $^{40-42}$S, $^{44-48}$Ar and $^{48-52}$Ca emitted from various californium isotopes. These plots are also found to be linear. We would like to point out that Geiger–Nuttal law is for

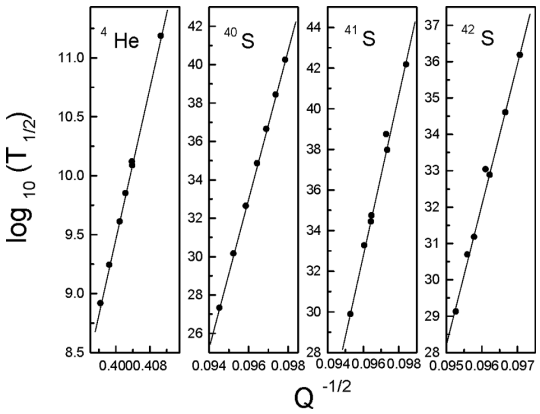

Figure 15. Geiger–Nuttal plots of $\log_{10}(T_{1/2})$ vs. $Q^{-1/2}$ for ^{4}He, $^{40-42}$S emitting from various californium isotopes.

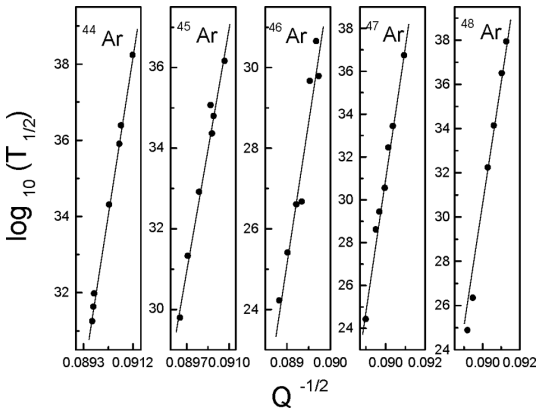

Figure 16. Geiger–Nuttal plots of $\log_{10}(T_{1/2})$ vs. $Q^{-1/2}$ for $^{44-48}$Ar emitting from various californium isotopes.

pure Coulomb potential but the inclusion of proximity potential does not produce much deviation to its linear nature, which agree with our earlier observations [22,35].

Figures 15–17 represent Geiger–Nuttal plots of $\log_{10}(T_{1/2})$ vs. $Q^{-1/2}$ for ^{4}He, $^{40-42}$S, $^{44-48}$Ar and $^{48-52}$Ca emitted from $^{248-254}$Cf isotopes. Geiger–Nuttal plots for all clusters are found to be linear with different slopes and intercepts. From the observed linear nature of these plots, we arrived at an equation for logarithm of half-life time as

$$\log_{10}(T_{1/2}) = \frac{X}{\sqrt{Q}} + Y. \tag{14}$$

The values of slope X and intercept Y for different clusters are given in table 4. Using the above equation we have calculated the half-life time for all clusters from various californium isotopes which are in good agreement with theoretical values.

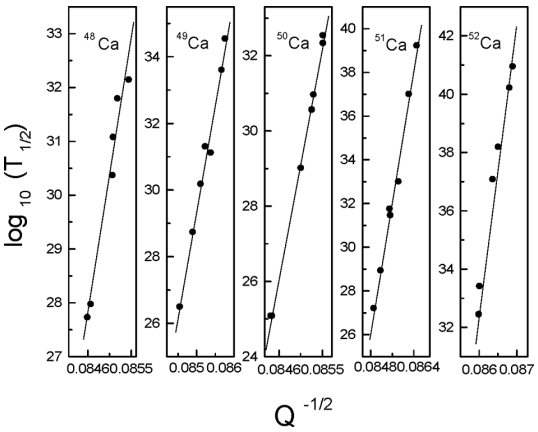

Figure 17. Geiger–Nuttal plots of $\log_{10}(T_{1/2})$ vs. $Q^{-1/2}$ for $^{48-52}$Ca emitting from various californium isotopes.

Acknowledgement

One of the authors (KPS) would like to thank University Grants Commission, Govt. of India for the financial support under project No. MRP(S)-352/2005(X Plan)/KLKA 002/UGC-SWRO.

References

[1] A Sandulescu, D N Poenaru and W Greiner, *Fiz. Elem. Chasitst. At. Yadra.* **11**, 1334 (1980) (*Sov. J. Part. Nucl.* **11**, 528 (1980))
[2] H J Rose and G A Jones, *Nature (London)* **307**, 245 (1984)
[3] R K Gupta and W Greiner, *Int. J. Mod. Phys.* **3**, 335 (1994)
[4] D N Poenaru, M Ivascu and A Sandulescu, *J. Phys.* **G5**, L169 (1979)
[5] R Blendowske, T Fliessbach and H Walliser, *Nucl. Phys.* **A464**, 75 (1987)
[6] D N Poenaru and W Greiner, *Phys. Scr.* **44**, 427 (1991)
[7] D N Poenaru and W Greiner, *J. Phys. G: Nucl. Part. Phys.* **17**, 443 (1991)
[8] D N Poenaru, W Greiner and E Hourani, *Phys. Rev.* **C51**, 594 (1995)
[9] K P Santhosh and Antony Joseph, *Pramana – J. Phys.* **59**, 599 (2002)
[10] R Bonetti and A Guglielmetti, in *Heavy elements and related new phenomena* edited by W Greiner and R K Gupta (World Scientific Publ., Singapore, 1999), vol. II, p. 643
[11] R K Gupta, in *Heavy elements and related new phenomena* edited by W Greiner and R K Gupta (World Scientific Publ., Singapore, 1999), vol. II, p. 730
[12] S Kumar and R K Gupta, *Phys. Rev.* **C49**, 1922 (1994)
[13] S Kumar, D Bir and R K Gupta, *Phys. Rev.* **C51**, 1762 (1995)
[14] S Kumar, J S Batra and R K Gupta, *J. Phys. G: Nucl. Part. Phys.* **22**, 215 (1996)
[15] A V Ramayya, J H Hamilton, L K Perker, J Kormick, B R S Babu, T N Ginter, A Sandulescu, A Florescu, F Carstoiu, W Greiner, G M Ter-Akopian, Yu Ts Oganessian, A V Daniel, W C Ma, P G Varmette, J O Rasmussen, S J Asztalos, S Y Chu, K E Gregorich, A O Macchiavelli, R W Macleod, J D Cole, R Aryaeinejad,K Butler-Moore, M WDrigert, M A Stoyer, L A Bernstein, R W Lougheed, K J Moody,

S G Prussin, S J Zhu, H C Griffin and R Donangelo, *Nuovo Cimento* **A110**, 1073 (1997)
[16] F Gonnenwein, A Moller, M Croni, M Hesse, M Wostheiarich, H Faust, G Fioni and S Oberstedt, *Nuovo Cimento* **A110**, 1089 (1997)
[17] A Moller, M Croni, F Gonnenwein and G Petrov, in *Proceedings of the International Conference on Large Amplitude Motion of Nuclei* edited by C Giardina (Brolo, Italy, 1996)
[18] A Sandulescu, A Florescu, F Carstoiu, A V Ramayya, J H Hamilton, J K Hwang, B R S Babu and W Greiner, *Nuovo Cimento* **A110**, 1079 (1997)
[19] A Sandulescu, A Florescu, F Carstoiu, W Greiner, J H Hamilton, A V Ramayya and B R S Babu, *Phys. Rev.* **C54**, 258 (1996)
[20] A Sandulescu and W Greiner, *J. Phys.* **G3**, 489 (1977)
[21] A V Ramayya, J H Hamilton, J K Hwang, L K Peker, J Kprmicki, B R S Babu, T N Ginter, A Sandulescu, A Florescu, F Carstoiu, W Greiner, G M Ter-Akopian, Yu Ts Oganessian, A V Daniel, W C Ma, P G Varmitte, J O Rasmussen, S J Asztalos, S Y Chu, K E Gregorich, A O Macchiavelli, R W Macleod, J D Cole, R Aryaeinejad, K Butler-Moore, M W Drigert, M A Stoyer, L A Bernstein, R W Lougheed, K J Moody, S G Prussin, S J Zhu, H C Griffin, and R Donangelo, *Phys. Rev.* **C57**, 2370 (1998).
[22] K P Santhosh and Antony Joseph, *Pramana – J. Phys.* **55**, 375 (2000)
[23] J Blocki, J Randrup, W J Swiatecki and C F Tsang, *Ann. Phys (N.Y.)* **105**, 427 (1977)
[24] J Blocki and W J Swiatecki, *Ann. Phys (N.Y.)* **132**, 53 (1981)
[25] D N Poenaru, M Ivascu, A Sandulescu and W Greiner, *Phys. Rev.* **C32**, 572 (1985)
[26] G Audi and A H Wapstra, *Nucl. Phys.* **A595**, 409 (1995)
[27] Y J Shi and W J Swiatecki, *Nucl. Phys.* **A438**, 450 (1985); **A464**, 205 (1987)
[28] S S Malik and R K Gupta, *Phys. Rev.* **C39**, 1992 (1989)
[29] G Royer, *J. Phys. G: Nucl. Part. Phys.* **26**, 1149 (2000)
[30] P B Price, R Bonetti, A Guglielmetti, C Chiesa, R Matheoud, C Migliono and K J Moody, *Phys. Rev.* **C46**, 1939 (1992)
[31] M Balasubramaniam and R K Gupta, *Phys. Rev.* **C60**, 064316 (1999)
[32] D N Basu, *Phys. Rev.* **C66**, 027601 (2002)
[33] P Moller, J R Nix, W D Myers and W Swiatecki, *At. Data Nucl. Data Tables* **59**, 185 (1995)
[34] S Wang, D Snowden-Ifft, P B Price, K J Moody and E K Hulet, *Phys Rev.* **C39**, 1647 (1989)
[35] K P Santhosh and Antony Joseph, *Pramana – J. Phys.* **58**, 611 (2002)